

11. B. Hönisch et al., *Science* **335**, 1058–1063 (2012).
12. C. L. Blättler, H. C. Jenkyns, L. M. Reynard, G. M. Henderson, *Earth Planet. Sci. Lett.* **309**, 77–88 (2011).
13. P. B. Wignall, S. Kershaw, P. Y. Collin, S. Crasquin-Soleau, *Geol. Soc. Am. Bull.* **121**, 954–956 (2009).
14. R. A. Berner, *Proc. Natl. Acad. Sci. U.S.A.* **99**, 4172–4177 (2002).
15. M. R. Rampino, K. Caldeira, *Terra Nova* **17**, 554–559 (2005).
16. W. S. Broecker, S. Peacock, *Global Biogeochem. Cycles* **13**, 1167–1172 (1999).
17. Materials and methods are available on Science Online
18. M. O. Clarkson et al., *Gondwana Res.* **24**, 233–242 (2013).
19. M. M. Joachimski, L. Simon, R. van Geldern, C. Lecuyer, *Geochim. Cosmochim. Acta* **69**, 4035–4044 (2005).
20. The alternative way to drive an increase in pH would be through a removal of carbon; however, this would be evident in the $\delta^{13}\text{C}$ record, so we can rule it out.
21. Bacterial sulfate reduction (BSR) is a net source of alkalinity if the generated H_2S is buried as pyrite. Pyrite deposition is seen widely in certain settings during the Late Permian to PTB. Further information is provided in the supplementary materials.
22. M. M. Joachimski et al., *Geology* **40**, 195–198 (2012).
23. H. Yin et al., *Earth Sci. Rev.* **137**, 19–33 (2014).
24. P. B. Wignall, R. J. Twitchett, in *Catastrophic Events and Mass Extinctions: Impacts and Beyond*, C. Koerber, K. G. MacLeod, Eds. (Geological Society of America, Boulder, CO, 2002), pp. 395–413.
25. C. Korte et al., *J. Asian Earth Sci.* **37**, 293–311 (2010).
26. H. Svensen et al., *Earth Planet. Sci. Lett.* **277**, 490–500 (2009).
27. E. S. Krull, G. J. Retallack, *Geol. Soc. Am. Bull.* **112**, 1459–1472 (2000).
28. A. D. Woods, *Earth Sci. Rev.* **137**, 6–18 (2013).
29. T. J. Algeo, Z. Q. Chen, M. L. Fraiser, R. J. Twitchett, *Palaeogeogr. Palaeoclimatol. Palaeoecol.* **308**, 1–11 (2011).
30. B. A. Black, J. F. Larmarque, C. A. Shields, L. T. Elkins-Tanton, J. T. Kiehl, *Geology* **42**, 67–70 (2014).
31. A. Baud, S. Richoz, S. Pruss, *Global Planet. Change* **55**, 81–89 (2007).
32. S. Richoz et al., *J. Asian Earth Sci.* **39**, 236–253 (2010).
33. B. A. Black, L. T. Elkins-Tanton, M. C. Rowe, I. U. Peate, *Earth Planet. Sci. Lett.* **317**, 363–373 (2012).
34. C. Korte et al., *Int. J. Earth Sci.* **93**, 565–581 (2004).
35. G. M. Stampfli, G. D. Borel, *Earth Planet. Sci. Lett.* **196**, 17–33 (2002).
36. S. Z. Shen et al., *Earth Planet. Sci. Lett.* **375**, 156–165 (2013).
37. B. Koehler et al., *GeoArabia* **15**, 91–156 (2010).
38. F. Maurer, R. Martini, R. Rettori, H. Hillgartner, S. Cirilli, *GeoArabia* **14**, 125–158 (2009).

ACKNOWLEDGMENTS

M.O.C. acknowledges funding from the Edinburgh University Principal's Career Development Scholarship, the International Centre for Carbonate Reservoirs, and The Marsden Fund (U001314). R.A.W., T.M.L., and S.W.P. acknowledge support from the Natural Environment Research Council through the "Co-evolution of Life and the Planet" scheme (NE/I005978). T.M.L. and S.J.D. were supported by the Leverhulme Trust (RPG-2013-106). S.A.K. and A.M. acknowledge support from the German Research Foundation (Deutsche Forschungsgemeinschaft) Major Research Instrumentation Program INST 144/307-1. This is a contribution to IGCP 572, with S.R. sponsored for fieldwork by the Austrian National Committee (Austrian Academy of Sciences) for the International Geoscience Programme (IGCP). We are grateful to R. Newton and A. Thomas for helpful discussions, L. Krystyn for field assistance, F. Maurer for discussions on stratigraphy and providing photomicrographs, and B. Mills for assisting with model studies. Data are available online in the supplementary materials and at www.pangaea.de.

SUPPLEMENTARY MATERIALS

www.sciencemag.org/content/348/6231/229/suppl/DC1
Materials and Methods
Supplementary Text
Figs. S1 to S9
Tables S1 to S10
References (39–98)

8 October 2014; accepted 4 March 2015
10.1126/science.aaa0193

COMETARY FORMATION

Molecular nitrogen in comet 67P/Churyumov-Gerasimenko indicates a low formation temperature

M. Rubin,^{1*} K. Altwegg,^{1,2} H. Balsiger,¹ A. Bar-Nun,³ J.-J. Berthelier,⁴ A. Bieler,^{1,5} P. Bochsler,¹ C. Briois,⁶ U. Calmonte,¹ M. Combi,⁵ J. De Keyser,⁷ F. Dhooghe,⁷ P. Eberhardt,^{1,†} B. Fiethe,⁸ S. A. Fuselier,⁹ S. Gasc,¹ T. I. Gombosi,⁵ K. C. Hansen,⁵ M. Hässig,^{1,9} A. Jäckel,¹ E. Kopp,¹ A. Korth,¹⁰ L. Le Roy,² U. Mall,¹⁰ B. Marty,¹¹ O. Mousis,¹² T. Owen,¹³ H. Rème,^{14,15} T. Sémon,¹ C.-Y. Tzou,¹ J. H. Waite,⁹ P. Wurz¹

Molecular nitrogen (N_2) is thought to have been the most abundant form of nitrogen in the protosolar nebula. It is the main N-bearing molecule in the atmospheres of Pluto and Triton and probably the main nitrogen reservoir from which the giant planets formed. Yet in comets, often considered the most primitive bodies in the solar system, N_2 has not been detected. Here we report the direct in situ measurement of N_2 in the Jupiter family comet 67P/Churyumov-Gerasimenko, made by the Rosetta Orbiter Spectrometer for Ion and Neutral Analysis mass spectrometer aboard the Rosetta spacecraft. A N_2/CO ratio of $(5.70 \pm 0.66) \times 10^{-3}$ (2σ standard deviation of the sampled mean) corresponds to depletion by a factor of $\sim 25.4 \pm 8.9$ as compared to the protosolar value. This depletion suggests that cometary grains formed at low-temperature conditions below ~ 30 kelvin.

Thermochemical models of the protosolar nebula (PSN) suggest that molecular nitrogen (N_2) was the principal nitrogen species during the disk phase (1) and that the nitrogen present in the giant planets was accreted in this form (2). Moreover, Pluto and Triton, which are both expected to have formed in the same region of the PSN as Jupiter family comets (JFCs), have N_2 -dominated atmospheres

and surface deposits of N_2 ice (3, 4). This molecule has never been firmly detected in comets; however, CN, HCN, NH, NH_2 , and NH_3 among others have been observed spectroscopically (5, 6). The abundance of N_2 in comets is therefore a key to understanding the conditions in which they formed.

Condensation or trapping of N_2 in ice occurs at similar thermodynamic conditions as those needed for CO in the PSN (7, 8). This requires very low PSN temperatures and implies that the detection of N_2 in comets and its abundance ratio with respect to CO would put strong constraints on comet formation conditions (7, 8). Ground-based spectroscopic observations of the N_2^+ band in the near ultraviolet are very difficult because of the presence of telluric N_2^+ and other cometary emission lines. Searches conducted with high-resolution spectra of comets 122P/de Vico, C/1995 O1 (Hale-Bopp), and 153P/2002 C1 (Ikeya-Zhang) have been unsuccessful and yielded upper limits of 10^{-5} to 10^{-4} for the N_2^+/CO^+ ratio (9, 10). Only one N_2^+ detection in C/2002 VQ94 (LINEAR) from ground-based observations is convincing, because the comet was at sufficient distance from the Sun to prevent terrestrial twilight N_2^+ contamination (11). The in situ measurements made by Giotto in 1P/Halley were inconclusive, because the resolution of the mass spectrometers aboard the spacecraft (12) was insufficient to separate the nearly identical masses of N_2 and CO during the 1P/Halley encounter, and only an upper limit could be derived for the relative production rates [$Q(\text{N}_2)/Q(\text{CO}) \leq 0.1$] (13).

Here we report the direct in situ measurement of the N_2/CO ratio by the Rosetta Orbiter Spectrometer for Ion and Neutral Analysis (ROSINA)

¹Physikalisches Institut, University of Bern, Sidlerstrasse 5, CH-3012 Bern, Switzerland. ²Center for Space and Habitability, University of Bern, Sidlerstrasse 5, CH-3012 Bern, Switzerland. ³Department of Geoscience, Tel-Aviv University, Ramat-Aviv, Tel-Aviv, Israel. ⁴Laboratoire Atmosphères, Milieux, Observations Spatiales (LATMOS)/Institut Pierre Simon Laplace-CNRS-UPMC-UVSQ, 4 Avenue de Neptune F-94100, Saint-Maur, France. ⁵Department of Atmospheric, Oceanic and Space Sciences, University of Michigan, 2455 Hayward, Ann Arbor, MI 48109, USA. ⁶Laboratoire de Physique et Chimie de l'Environnement et de l'Espace (LPC2E), UMR 6115 CNRS-Université d'Orléans, Orléans, France. ⁷Belgian Institute for Space Aeronomy, Belgisch Instituut voor Ruimte-Aeronomie-Instituut d'Aéronomie Spatiale de Belgique (BIRA-IASB), Ringlaan 3, B-1180 Brussels, Belgium. ⁸Institute of Computer and Network Engineering, Technische Universität Braunschweig, Hans-Sommer-Strasse 66, D-38106 Braunschweig, Germany. ⁹Department of Space Science, Southwest Research Institute, 6220 Culebra Road, San Antonio, TX 78228, USA. ¹⁰Max-Planck-Institut für Sonnensystemforschung, Justus-von-Liebig-Weg 3, 37077 Göttingen, Germany. ¹¹Centre de Recherches Pétrographiques et Géochimiques (CRPG)-CNRS, Université de Lorraine, 15 rue Notre Dame des Pauvres, Boîte Postale 20, 54501 Vandœuvre lès Nancy, France. ¹²Aix Marseille Université, CNRS, Laboratoire d'Astrophysique de Marseille UMR 7326, 13388, Marseille, France. ¹³Institute for Astronomy, University of Hawaii, Honolulu, HI 96822, USA. ¹⁴Université de Toulouse: UPS-OMP; Institut de Recherche en Astrophysique et Planétologie (IRAP), Toulouse, France. ¹⁵CNRS; IRAP; 9 Avenue du Colonel Roche, Boîte Postale 44346, F-31028 Toulouse Cedex 4, France.

*Corresponding author. E-mail: martin.rubin@space.unibe.ch
†Deceased.

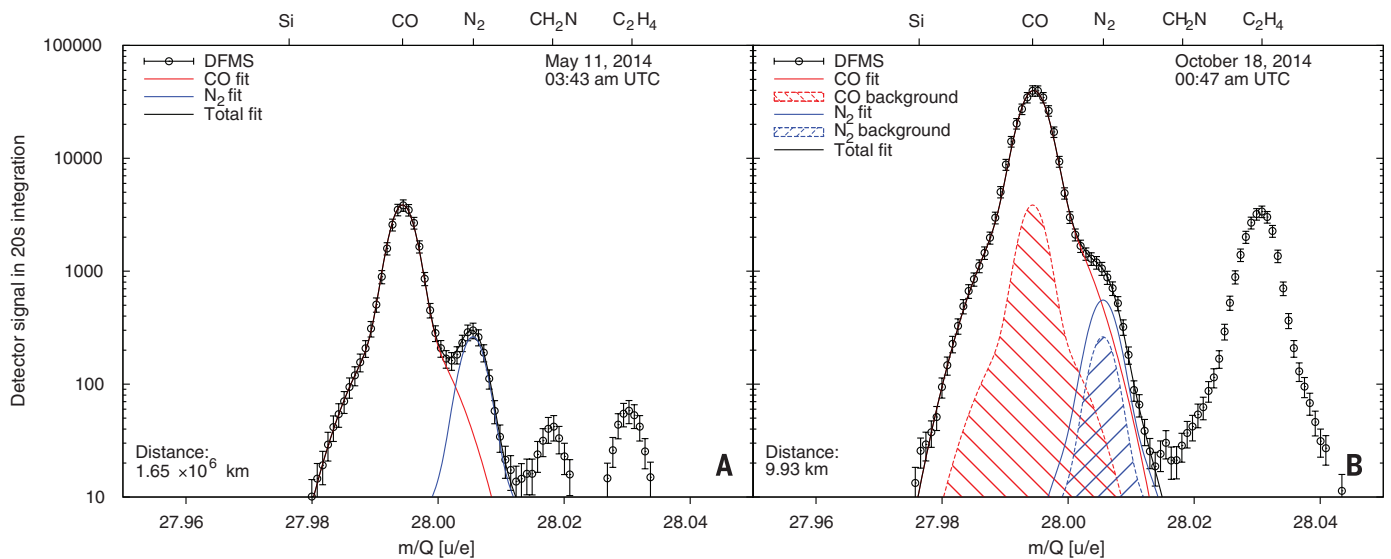


Fig. 1. Mass per charge 28 u/e spectra before (A) and after (B) entering the coma of 67P, including statistical and 10% pixel gain error. (A) was obtained in May 2014 and (B) is a representative spectrum from October containing the sum of the cometary parents and fragments and the spacecraft background signals.

in the JFC 67P/Churyumov-Gerasimenko (hereafter 67P). ROSINA is the mass spectrometer suite on the European Space Agency's Rosetta spacecraft (14) and measures the gas density and composition at the location of the spacecraft (15). The Double Focusing Mass Spectrometer (DFMS) has a high mass resolution of $m/\Delta m$ about 3000 at the 1% level (corresponding to ~ 9000 half peak width at the 50% level) at atomic mass per unit of charge 28 u/e, allowing the separation of N_2 from CO ($\Delta m = 0.011$ u) by numerical peak fitting. Neutral gas is ionized by electron impact and then deflected through an electrostatic, then magnetic, filter onto a position-sensitive microchannel plate (MCP) detector. The peak shape of a single species on the MCP is well known, and therefore numerical fitting can distinguish overlapping contributions from different atoms and molecules (see the supplementary materials).

Starting on 5 August 2014, ROSINA observed the cometary gas flux rise above the spacecraft background signal for the major species, including H_2O , CO, and CO_2 . For N_2 , which has a higher relative spacecraft background, the cometary signal became apparent a few days later. The spacecraft background signal (16) for both species, CO and N_2 , was derived at different times before detecting the coma and shown to be temporally quite stable. N_2 and CO were both observed in the Rosetta spacecraft background mass spectra, e.g., on 11 May 2014, while the spacecraft was still at a distance of 1.65×10^6 km from the comet (Fig. 1A). A comparable N_2 background was measured on 1 August 2014, at almost 800 km from the nucleus before the cometary signal became apparent. Another mass spectrum, representative of the measurements within a distance of 10 km from the nucleus, was obtained on 18 October 2014 (Fig. 1B) and includes both cometary and spacecraft background signal. The indicated background was subsequently removed, leaving only cometary CO and N_2 . Furthermore, CO from dissociative electron-impact ionization of cometary CO_2 inside DFMS' ion source was removed (a 7 to 36% reduction), and the signal was corrected for the instrument alignment with respect to the comet (supplementary materials).

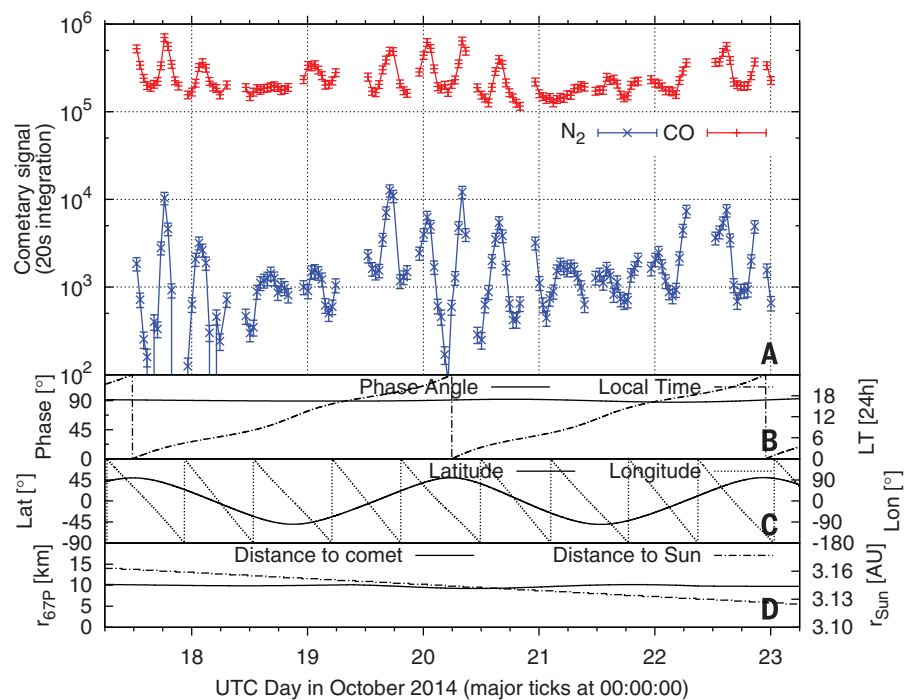


Fig. 2. Cometary parent CO and N_2 signal during 17 to 23 October 2014. (A) The error bars are associated with the accuracy of the fit, background subtraction, detector gain, and statistical error. Gaps in the data indicate times when ROSINA was off due to thruster operations. The sections below show phase angle and local time (B), latitude and longitude of the subspacecraft point (C) in the Cheops coordinate system, and the distances of Rosetta to the comet (r_{67P}) and the comet to the Sun (r_{Sun}) (D). The summer hemisphere is at positive latitudes.

This procedure was carried out for 138 spectra over two terminator orbits of the Rosetta spacecraft from 17 to 23 October 2014. Clear diurnal variations in the cometary signal of both species associated with the 12.4-hour rotation period of the comet have been observed (Fig. 2A).

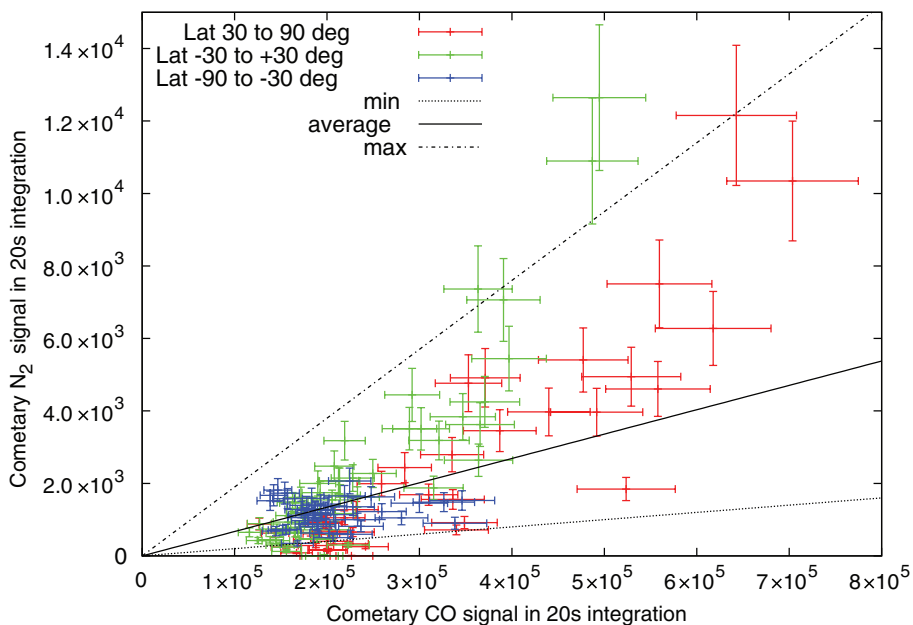


Fig. 3. Cometary parent N_2 versus CO signal. The min and max lines bracket most measurements. To derive the N_2/CO ratio, the detector signal ratio in the plot has to be divided by the differential sensitivity of 1.175. The average N_2/CO ratio of 5.70×10^{-3} is given by the solid black line; the min and the max lines show the observed variation and correspond to ratios of 1.7×10^{-3} and 1.6×10^{-2} .

The signal is to first order correlated to the comet's cross-section exposed to the Sun and the relative position of Rosetta (Fig. 2, B to D). The resulting mean N_2/CO ratio of $(5.70 \pm 0.66) \times 10^{-3}$ in the observed time period corresponds to the mean ratio of each individual measurement and includes the 2σ SD of the sampled mean. Higher outgassing is found at positive latitudes corresponding to the summer hemisphere. Over the sunlit hemisphere, the CO/H_2O ratio varies between 0.1 to 0.3 (17), which is in agreement with variations observed at other comets (6). Because these measurements were achieved at a heliocentric distance of 3.1 astronomical units (AU), the water production rate may increase relative to both CO and N_2 as the comet approaches the Sun. We therefore expect the N_2/CO ratio to be more representative of the N_2 content in the coma than the N_2/H_2O ratio. The N_2/CO ratio exhibits a strong variation depending on the position of Rosetta above the surface of the comet nucleus between 0.17 to 1.6% (Fig. 3). There are also hints of a nonlinear relationship between N_2 and CO, further indicating that thermal processes in the upper layer of the nucleus and/or surface inhomogeneities might influence the measured N_2/CO ratio in the coma.

With a protosolar ratio N/C of 0.29 ± 0.10 (18) and assuming to first order that all of N and C were in the form of N_2 and CO in the PSN (1), we derived an N_2/CO ratio of 0.145 ± 0.048 in the PSN gas phase. The comparison with the N_2/CO measurement performed in the near coma of 67P shows that the cometary N_2/CO ratio is depleted by a factor of about 25.4 ± 8.9 as compared to the value derived from protosolar N and C abun-

dances. This depletion of N_2 relative to CO in comet 67P may be a consequence of how cometary ice formed. According to one model, comets agglomerated from pristine amorphous water ice grains originating from the interstellar medium (ISM) (19). In this case, the low N_2/CO ratio in 67P is the result of inefficient trapping of N_2 in amorphous water ice as compared to CO. This possibility is supported by laboratory experiments in which a mixture of water vapor with N_2 and CO was directed onto a cold plate in the 24 to 30 K temperature range (7). In these experiments, gases initially trapped in growing amorphous ice were later released when ice warmed up, and the evolved gases were measured by mass spectrometry. At 24 K, the depletion factor for the N_2/CO ratio was found to be ~ 19 , a value within the range of the one observed in 67P of 25.4 ± 8.9 . This yields a lower limit for the temperature experienced by the grains agglomerated by 67P, because the N_2/CO ratio in amorphous ice would increase at temperatures lower than 24 K because of increasing efficiency of N_2 trapping.

An alternative interpretation of the low N_2 abundance is that 67P agglomerated from grains consisting of clathrates, which are icelike crystalline solids formed by cages of water molecules that contain small nonpolar molecules (20). This hypothesis is based on models showing that the vaporization distance of ISM ices could have been as high as about 30 AU from the Sun when they entered the PSN (21). With time, the decrease of the gas temperature and pressure allowed water to condense at ~ 140 to 150 K in the form of crystalline ice, leaving negligible water in the gas phase to condense at low temperatures where

amorphous ice is expected to form (22). Depending on the nature of the entrapped species, clathrates formed from preexisting crystalline water ice when the PSN temperature was lower than about 80 K, provided that the slow kinetics of the process was balanced by sufficient formation time (8). As in the case of trapping in amorphous ice, experiments and models suggest that N_2 is poorly trapped in clathrate cages, because of its small size (8, 23–25). In particular, statistical thermodynamics models (26) used to compute the composition of clathrates formed from a protosolar-composition gas in the PSN show that an N_2/CO ratio in the comet's nucleus is consistent with the measured value in the coma if the nucleus agglomerated from grains formed in the 26 to 56 K temperature range (8).

Both interpretations are consistent with the idea that 67P agglomerated from grains formed at about 30 K or below. However, the measured N_2/CO ratio may reflect in whole or in part the comet's post-formation evolution. A possibility is that 67P agglomerated from grains formed at a lower temperature (around 20 K) in the PSN, favoring the trapping of much more N_2 in its building blocks, in a way consistent with the known compositions of the atmospheres and surfaces of Pluto and Triton (3, 4). This possibility would be consistent with an inferred Kuiper Belt origin for 67P and its high D/H ratio (27). In these conditions, 67P could have been initially N_2 -rich but subsequent post-accretion heating due to the radiogenic decay of nuclides and/or thermal cycles during its transit from the Kuiper Belt and its subsequent history in a short period orbit could have been sufficient to trigger the outgassing of N_2 (8). A scenario such as this may explain how initial nitrogen-rich cometsimals similar to Triton and Pluto evolved into nitrogen-depleted comets.

Because N_2 trapped in 67P is presumably PSN gas, its $^{14}N/^{15}N$ ratio should be about 441, the value found in Jupiter and the solar wind (28). This is much higher than values measured in other cometary N-bearing species such as NH_3 and HCN (~ 130) (5). Thus, depending on the proportions of N_2 relative to other N-bearing species, the terrestrial $^{14}N/^{15}N$ ratio of 272 could possibly be cometary in origin, given an appropriate mix of the different nitrogen species in the comets that contributed to terrestrial volatiles (e.g., $\sim 50\%$ N_2 and $\sim 50\%$ NH_3 or HCN). Our initial ROSINA measurement for N_2/CO of 0.57% may be compared with NH_3/CO of 6% and HCN/CO of $\sim 2\%$ in the Oort cloud comet Hale-Bopp (6). The production rates of volatiles relative to water vary from one comet to another, but their values normalized to CO remain close to those measured in Hale-Bopp (6). If 67P is a typical JFC, then the ROSINA value for N_2/CO implies that the amount of N_2 reaching the surface of a solid body in the inner solar system from a JFC impact was almost 15 times less than the amounts of NH_3 , HCN, and certain organic compounds (6). This comparison suggests that JFC comets were not the main source of Earth's nitrogen.

REFERENCES AND NOTES

1. B. J. Fegley, R. G. Prinn, in *The Formation and Evolution of Planetary Systems*, H. A. Weaver et al., Eds. (Univ. of Arizona Press, Tucson, AZ, 1989), pp. 171–205.
2. O. Mousis et al., *Planet. Space Sci.* **104**, 29–47 (2014).
3. D. P. Cruikshank et al., *Science* **261**, 742–745 (1993).
4. T. C. Owen et al., *Science* **261**, 745–748 (1993).
5. P. Rousselot et al., *Astrophys. J.* **780**, L17 (2014).
6. D. Bockelée-Morvan et al., in *Comets II*, M. Festou, H. U. Keller, H. A. Weaver, Eds. (Univ. of Arizona Press, Tucson, AZ, 2004), pp. 391–423.
7. A. Bar-Nun, G. Notesco, T. Owen, *Icarus* **190**, 655–659 (2007).
8. O. Mousis et al., *Astrophys. J.* **757**, 146 (2012).
9. A. L. Cochran, W. D. Cochran, E. S. Barker, *Icarus* **146**, 583–593 (2000).
10. A. L. Cochran, *Astrophys. J.* **576**, L165–L168 (2002).
11. P. P. Korsun, P. Rousselot, I. V. Kulyk, V. L. Afanasiev, O. V. Ivanova, *Icarus* **232**, 88–96 (2014).
12. D. Krankowsky et al., *Nature* **321**, 326–329 (1986).
13. P. Eberhardt et al., *Astron. Astrophys.* **187**, 481–484 (1987).
14. K.-H. Glassmeier, H. Boehnhardt, D. Koschny, E. Kürt, I. Richter, *Space Sci. Rev.* **128**, 1–21 (2007).
15. H. Balsiger et al., *Space Sci. Rev.* **128**, 745–801 (2007).
16. B. Schlappi et al., *J. Geophys. Res. Space Phys.* **115**, A12313 (2010).
17. M. Hässig et al., *Science* **347**, aaa0276 (2015).
18. K. Lodders, H. Palme, H. P. Gail, in *The Solar System*, J. E. Trümper, Ed. (Springer-Verlag, Berlin Heidelberg, 2009), vol. 4B.
19. T. Owen, A. Bar-Nun, *Nature* **361**, 693–694 (1993).
20. O. Mousis et al., *Icarus* **148**, 513–525 (2000).
21. K. M. Chick, P. Cassen, *Astrophys. J.* **477**, 398–409 (1997).
22. A. Kouchi, T. Yamamoto, T. Kozasa, T. Kuroda, J. M. Greenberg, *Astron. Astrophys.* **290**, 1009–1018 (1994).
23. J.-M. Herri, E. Chassefière, *Planet. Space Sci.* **73**, 376–386 (2012).
24. D. E. Sloan, C. Koh, *Clathrate Hydrates of Natural Gases* (CRC/Taylor & Francis, Boca Raton, FL, ed. 3, 2007).
25. N. Iro, D. Gautier, F. Hersant, D. Bockelée-Morvan, J. I. Lunine, *Icarus* **161**, 511–532 (2003).
26. J. I. Lunine, D. J. Stevenson, *Astrophys. J.* **58**, 493–531 (1985).
27. K. Altwegg et al., *Science* **347**, 1261952 (2015).
28. B. Marty, M. Chaussidon, R. C. Wiens, A. J. G. Jurewicz, D. S. Burnett, *Science* **332**, 1533–1536 (2011).

ACKNOWLEDGMENTS

The authors thank the following institutions and agencies, which supported this work: Work at the University of Bern was funded by the State of Bern, the Swiss National Science Foundation, and the European Space Agency PRODEX Program. Work at the Max Planck Institute for Solar System Research was funded by the Max-Planck Society and Bundesministerium für Wirtschaft und Energie under contract 50QPI302. Work at the Southwest Research Institute was supported by subcontract no. 1496541 from the Jet Propulsion Laboratory (JPL). Work at BIRA-IASB was supported by the Belgian Science Policy Office via PRODEX/ROSINA PEA 90020. This work has been carried out thanks to the support of the A*MIDEX project (no. ANR-11-IDEX-0001-02) funded by the “Investissements d’Avenir” French government program, managed by the French National Research Agency (ANR). This work was supported by CNES grants at IRAP; LATMOS; LPC2E; Univers, Transport, Interfaces, Nanostructures, Atmosphère et Environnement, Molécules (UTINAM); and CRPG and by the European Research Council (grant no. 267255 to B.M.). A.B.-N. thanks the Ministry of Science and the Israel Space Agency. Work at the University of Michigan was funded by NASA under contract JPL-1266313. Work by J.H.W. at the Southwest Research Institute was funded by NASA JPL subcontract NAS703001TONM0710889. The results from ROSINA would not be possible without the work of the many engineers, technicians, and scientists involved in the mission, in the Rosetta spacecraft, and in the ROSINA instrument team over the past 20 years, whose contributions are gratefully acknowledged. We thank herewith the work of the whole European Space Agency (ESA) Rosetta team. Rosetta is an ESA mission with contributions from its member states and NASA. All ROSINA data are available on request until they are released to the Planetary Science Archive of ESA and the Planetary Data System archive of NASA.

SUPPLEMENTARY MATERIALS

www.sciencemag.org/content/348/6231/232/suppl/DC1
Materials and Methods

12 January 2015; accepted 3 March 2015
Published online 19 March 2015;
10.1126/science.aaa6100

HUMAN GENETICS

Common variants spanning *PLK4* are associated with mitotic-origin aneuploidy in human embryos

Rajiv C. McCoy,¹ Zachary Demko,² Allison Ryan,² Milena Banjevic,² Matthew Hill,² Styrmir Sigurjonsson,² Matthew Rabinowitz,² Hunter B. Fraser,¹ Dmitri A. Petrov¹

Aneuploidy, the inheritance of an atypical chromosome complement, is common in early human development and is the primary cause of pregnancy loss. By screening day-3 embryos during in vitro fertilization cycles, we identified an association between aneuploidy of putative mitotic origin and linked genetic variants on chromosome 4 of maternal genomes. This associated region contains a candidate gene, *Polo-like kinase 4 (PLK4)*, that plays a well-characterized role in centriole duplication and has the ability to alter mitotic fidelity upon minor dysregulation. Mothers with the high-risk genotypes contributed fewer embryos for testing at day 5, suggesting that their embryos are less likely to survive to blastocyst formation. The associated region coincides with a signature of a selective sweep in ancient humans, suggesting that the causal variant was either the target of selection or hitchhiked to substantial frequency.

Deviation from a balanced chromosome complement, a phenomenon known as aneuploidy, is common in early human embryos and often leads to embryonic mortality (1). Approximately 75% of embryos are at least partially aneuploid by day 3 because of prevalent errors of both meiotic and postzygotic origin (2, 3), and this proportion increases with maternal age (1). The propensity to produce aneuploid embryos varies substantially, however, even among mothers of a similar age (4). We therefore hypothesized that variation in parents’ genomes may explain variation in aneuploidy incidence. We tested this hypothesis by performing a genome-wide association study of aneuploidy risk among patients undergoing pre-implantation genetic screening (PGS) of embryos collected from in vitro fertilization (IVF) cycles.

Embryo DNA (single-cell day-3 blastomere biopsies or multicell day-5 trophoctoderm biopsies) and parent DNA were genotyped on a single-nucleotide polymorphism (SNP) microarray (5). The Parental Support algorithm (6) was then applied to determine the chromosome-level ploidy status of each embryo sample. This algorithm overcomes high rates of allelic dropout and other quality limitations of whole-genome amplification by supplementing these data with high-quality genotypes from parental chromosomes. The copy number of each embryonic chromosome can then be inferred by comparing microarray channel intensities from DNA amplified from the embryo biopsy to those expected given the parental genotypes at each marker. Combining these fine-scale observations across large chromosomal windows facilitates the detection of particular forms of aneuploidy and the assignment of copy number variations to specific parental homologs (6).

Previous validation has been performed for individual blastomeres (6), so it is unknown how accuracy would be affected in the face of chromosomal mosaicism that could potentially affect multicell trophoctoderm biopsies. We therefore performed an association study on 2362 unrelated mothers (1956 IVF patients and 406 oocyte donors) and 2360 unrelated fathers meeting genotype quality-control thresholds (5) and from whom at least one day-3 biopsy was obtained, with the blastomere providing a high-confidence result (a total of 20,798 blastomeres). We then separately analyzed the additional 15,388 trophoctoderm biopsies to gain insight into selection occurring before this developmental stage.

We first tested for associations between the rates of errors of putative maternal meiotic origin (fig. S1) (5) and maternal genotypes, identifying no association achieving genome-wide significance (logistic GLM, *P*-value threshold = 5×10^{-8}). We next tested for associations between the rates of errors of putative mitotic origin and parental genotypes. The first mitotic divisions of the developing embryo take place under the control of maternal gene products provided to the oocyte (7) and are substantially error-prone (2, 3). We hypothesized that variation in maternal gene products may thus contribute to variation in rates of postzygotic error among embryos from different mothers. To encode the mitotic error phenotype, we designated all blastomeres with aneuploidies affecting a paternal chromosome copy (excluding paternal trisomies of putative meiotic origin) as cases, and all other blastomere samples as controls (Fig. 1A). Because aneuploidy has been estimated to affect fewer than 5% of sperm (8) and because paternal meiotic trisomies were detected for fewer than 1% of the blastomeres in our data, this set of aneuploid cases should be nearly exclusively mitotic in origin.

¹Department of Biology, Stanford University, Stanford, CA, USA. ²Natera, Inc., San Carlos, CA, USA.



http://www.rndsystems.com/rnd_page_objectname_sample_size_antibodies.aspx?utm_source=Science.com&utm_medium=PDF&utm_campaign=SampleSizeAntibodies



Molecular nitrogen in comet 67P/Churyumov-Gerasimenko indicates a low formation temperature

M. Rubin *et al.*

Science **348**, 232 (2015);

DOI: 10.1126/science.aaa6100

This copy is for your personal, non-commercial use only.

If you wish to distribute this article to others, you can order high-quality copies for your colleagues, clients, or customers by [clicking here](#).

Permission to republish or repurpose articles or portions of articles can be obtained by following the guidelines [here](#).

The following resources related to this article are available online at www.sciencemag.org (this information is current as of April 13, 2015):

Updated information and services, including high-resolution figures, can be found in the online version of this article at:

<http://www.sciencemag.org/content/348/6231/232.full.html>

Supporting Online Material can be found at:

<http://www.sciencemag.org/content/suppl/2015/03/18/science.aaa6100.DC1.html>

This article **cites 23 articles**, 5 of which can be accessed free:

<http://www.sciencemag.org/content/348/6231/232.full.html#ref-list-1>

This article appears in the following **subject collections**:

Astronomy

<http://www.sciencemag.org/cgi/collection/astronomy>

Planetary Science

http://www.sciencemag.org/cgi/collection/planet_sci